

Communication: Effects of stress on the tube confinement potential and dynamics of topologically entangled rod fluids

Daniel M. Sussman and Kenneth S. Schweizer

Citation: [The Journal of Chemical Physics](#) **135**, 131104 (2011); doi: 10.1063/1.3651143

View online: <http://dx.doi.org/10.1063/1.3651143>

View Table of Contents: <http://scitation.aip.org/content/aip/journal/jcp/135/13?ver=pdfcov>

Published by the [AIP Publishing](#)

Articles you may be interested in

[A constitutive model for entangled polymers incorporating binary entanglement pair dynamics and a configuration dependent friction coefficient](#)

J. Rheol. **59**, 335 (2015); 10.1122/1.4905921

[Stress in Next Generation Interconnects](#)

AIP Conf. Proc. **817**, 157 (2006); 10.1063/1.2173545

[Stress relaxation dynamics of an entangled polystyrene solution following step strain flow](#)

J. Rheol. **50**, 59 (2006); 10.1122/1.2135331

[Zero-shear stress relaxation and long time dynamics of a linear polyethylene melt: A test of Rouse theory](#)

J. Chem. Phys. **114**, 8685 (2001); 10.1063/1.1368135

[Stress Relaxation and Differential Dynamic Modulus of Polyisobutylene in Large Shearing Deformations](#)

J. Rheol. **29**, 273 (1985); 10.1122/1.549791

An advertisement for AIP Applied Physics Reviews. It features a blue background with a molecular structure of spheres and rods. On the left is a thumbnail image of the journal cover for 'AIP Applied Physics Reviews', which shows a 3D grid and a graph. The main text reads 'NEW Special Topic Sections' in large white letters. Below this, in orange text, it says 'NOW ONLINE' followed by 'Lithium Niobate Properties and Applications: Reviews of Emerging Trends'. The AIP Applied Physics Reviews logo is in the bottom right corner.

NEW Special Topic Sections

NOW ONLINE
Lithium Niobate Properties and Applications:
Reviews of Emerging Trends

AIP Applied Physics Reviews

Communication: Effects of stress on the tube confinement potential and dynamics of topologically entangled rod fluids

Daniel M. Sussman¹ and Kenneth S. Schweizer^{2,3,a)}

¹*Department of Physics, University of Illinois, Urbana, Illinois 61801, USA*

²*Departments of Materials Science, Chemistry and Chemical and Biomolecular Engineering, University of Illinois, Urbana, Illinois 61801, USA*

³*Frederick Seitz Materials Research Laboratory, University of Illinois, Urbana, Illinois 61801, USA*

(Received 31 August 2011; accepted 22 September 2011; published online 7 October 2011)

A microscopic theory for the effect of applied stress on the transverse topological confinement potential and slow dynamics of heavily entangled rigid rods is presented. The confining entanglement force localizing a polymer in a tube is predicted to have a finite strength. As a consequence, three regimes of terminal relaxation behavior are predicted with increasing stress: accelerated reptation due to tube widening (dilation), relaxation via deformation-assisted activated transverse barrier hopping, and complete destruction of the lateral tube constraints corresponding to microscopic yielding or a disentanglement transition. © 2011 American Institute of Physics. [doi:10.1063/1.3651143]

The response of high-molecular-weight, topologically entangled polymer melts and solutions to external deformations is a topic of great scientific interest in nonequilibrium statistical mechanics, and also of central importance in polymer processing, liquid-crystal dynamics, biophysics, and cell mechanics. Given the difficulty in creating a microscopic theory of quiescent entangled polymer dynamics, widely believed to be controlled by “topological constraints” arising from connectivity and uncrossability, it is not surprising that treating the nonlinear mechanical response is especially challenging.^{1,2} The most popular and well-developed approaches for linear macromolecules (chains, rods) are built on phenomenological ideas of deGennes and Doi-Edwards: single-chain dynamic theories in which inter-chain interactions are replaced *via ansatz* by an effective confining “tube” that strictly forbids large-scale displacement transverse to the polymer backbone.¹ Multiple corrections to the quiescent tube model are experimentally important, which enhance polymer mobility and reduce motional anisotropy.²

The extension of the reptation-tube model to treat nonlinear rheology requires additional uncontrolled approximations that are difficult to directly test. For example, for many years it was assumed that stress does not destroy tube confinement, corresponding to an analogy between physical entanglements in molten polymers and chemical crosslinks in a rubber network.¹ However, the qualitative failure of the tube model to properly describe shear thinning motivated the postulate of a “convective constraint release” (CCR) mechanism, whereby fast flows can sweep away entanglement constraints.^{2,3} Implementation of CCR (with adjustable parameter(s)) qualitatively improves the model with respect to experiment, but its microscopic basis at the level of forces remains unclear. Moreover, other complications of potentially qualitative importance have not been consistently addressed, e.g., recent simulations have found evidence for stress-induced tube widening (“dilation”) or reduction in en-

tanglement density.⁴ Additionally, experiments and qualitative arguments have suggested that stress can induce an “entanglement-disentanglement transition,”⁵ and that the confining tube can be strongly weakened or completely destroyed in analogy with a “yielding” event.⁶ Recent opinion pieces summarizing the state of understanding of entangled polymer dynamics have emphasized the need for a conceptual breakthrough, especially on the tube diameter scale and under strong deformation conditions.⁷

In this Communication, we initiate the extension of our first-principles microscopic approach for entangled polymer dynamics^{8,9} in a fluid of infinitely thin, non-rotating rigid rods of length L to treat the effect of applied stress. Our prior theory predicted the crossover to anisotropic diffusion and the full transverse confining field when the rod number density ρ (degree of entanglement) exceeds a critical threshold. Our central finding here is that confining tubes and entanglements can be massively weakened, and even destroyed, beyond a relatively modest level of stress or strain. This prediction has major implications for nonlinear relaxation and provides a microscopic basis for understanding the dramatic phenomena mentioned earlier.

Our starting point is the microscopic dynamic mean-field theory of Szamel for the entangled-needle fluid as a function of a single dimensionless coupling constant ρL^3 .¹⁰ If uncrossability is exactly enforced at the binary collision level and multiple correlated rod collisions are self-consistently renormalized, then for $\rho L^3 \gg 1$ the static tube-model scaling laws for the transverse diffusion constant, D_\perp , and a dynamic localization length (tube radius), r_l , are recovered. For heavily entangled rods the long-time rotational diffusion constant is proportional to its transverse analog, and the diffusion constant is inversely related to the terminal relaxation time.^{8–10} Hence, knowledge of D_\perp captures all long-time dynamics.

Recently, we qualitatively extended the Szamel approach to create a microscopic theory⁹ of the full dynamic confinement potential as a function of the instantaneous center-of-mass (CM) transverse displacement, r_\perp , with the result

^{a)}Electronic mail: kschweiz@illinois.edu.

$F_{dyn}(r_{\perp}) = -\int_{r_l}^{r_{\perp}} f(r)dr$, where

$$\frac{f(r)}{k_B T} = \frac{2}{r} - \frac{3\pi}{4} \frac{\rho}{\rho_c} \frac{g(L/r)}{r}. \quad (1)$$

Here, $g(x) = (x - I_1(2x) + \mathbf{L}_1(2x))/2x^2$, $\mathbf{L}_1(I_1)$ is the first Struve function (modified Bessel function of the first kind), and $\rho_c L^3 = 3\sqrt{2}$ is the critical reduced density at which a transverse barrier first emerges.^{8,9} The form of $F_{dyn}(r_{\perp})$ reflects a competition between a delocalizing entropic force and a localizing intermolecular entanglement force. Under quiescent conditions the confinement potential is infinitely deep but harmonic only up to $\sim 1 k_B T$, beyond which it initially grows roughly linearly with polymer displacement. This results in exponential tails in the rod displacement distribution function at intermediate times, in excellent accord⁹ with experiments on F-actin solutions.¹¹ For larger transverse displacements the confinement potential further softens, with tube confinement growing only logarithmically.

To include applied deformation at the single-particle CM level the stress-based “instantaneous Eyring” approach¹² is adopted, formulated within the nonlinear Langevin equation (NLE) framework we employed for quiescent entangled polymer dynamics.⁹ The stressed version of the NLE theory has been successfully applied to understand nonlinear relaxation and mechanics in colloidal and polymer glasses.^{12,13} The key idea is that an applied macroscopic stress, σ , results in a force on the polymer CM which weakens dynamical constraints. An equivalent physical picture is that F_{dyn} acquires a mechanical-work contribution that is linear in both stress and instantaneous transverse displacement: $F_{dyn}(r_{\perp}, \sigma) = F_{dyn}(r_{\perp}, \sigma = 0) - \pi L^2 \sigma r_{\perp} / 4$, where the relevant cross-sectional area is taken to be a circle of diameter L . Here, deformation is assumed to not modify the isotropic rod orientation distribution, a restriction relaxed below.

Figure 1 shows representative plots of the dramatic effect of stress on the tube confinement potential. The critical finding is that *any* nonzero value of σ destroys the infinitely deep nature of the confining field. This is a consequence of the predicted weak localization constraints at large displacements, $F_{dyn}(r_{\perp} > L) \sim (\rho/\rho_c - 2) \log(r_{\perp}/L)$,

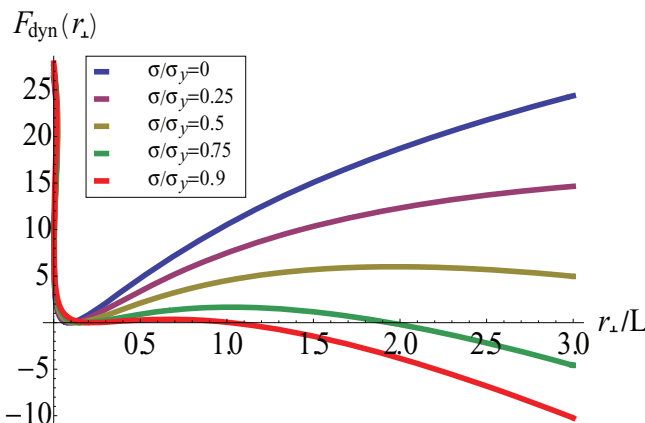


FIG. 1. Transverse confinement potential (in units of thermal energy) as a function of reduced transverse CM displacement at $\rho/\rho_c = 10$ as reduced stress increases (top to bottom).

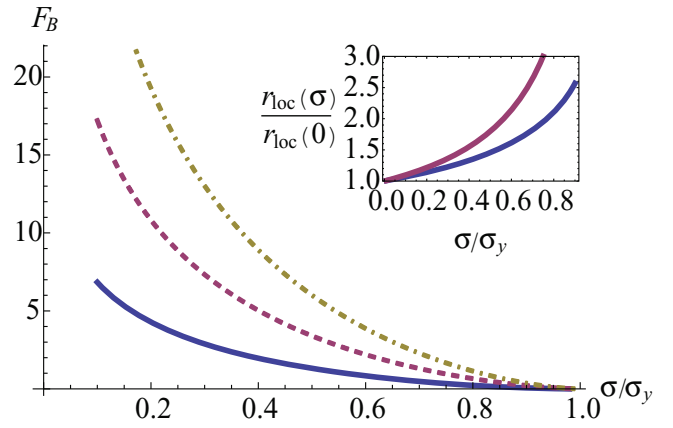


FIG. 2. Barrier height in units of $k_B T$ vs. normalized stress for $\rho/\rho_c = 3, 6, 10$ (bottom to top). Inset: normalized tube radius vs. normalized stress for $\rho/\rho_c = 10$ (lower curve) and $\rho/\rho_c = 100$ (upper). At these four densities, the estimated absolute yield strains are $\sigma_y/G_e \approx 0.28, 0.52, 0.67$, and 1.04 , respectively, with increasing density.

and the finite strength of the maximum quiescent confinement force, $f_{\max} \simeq 2k_B T/r_l = \pi k_B T \rho L^2 / 4\sqrt{2}$ for $\rho \gg \rho_c$.⁹ This latter feature implies that the tube is destroyed (entropic barrier height $F_B \rightarrow 0$) at an applied force or “absolute yield”^{12,13} stress of $\sigma_y = 4f_{\max}/\pi L^2 \simeq \rho k_B T / \sqrt{2}$. The corresponding microscopic yield strain can be estimated as $\gamma_y = \sigma_y/G_e$. Since the rod-solution shear modulus $G_e = 3\rho k_B T/5$, $\sigma_y = 5G_e/3\sqrt{2}$ and hence $\gamma_y \approx 1$ when $\rho \gg \rho_c$. For small stresses, additional features of $F_{dyn}(r_{\perp})$ can be analytically derived when $\rho \gg \rho_c$: the tube radius grows with stress as $r_l(\sigma)/r_l(0) \approx (1 - \tilde{\sigma}/3(\rho/\rho_c))^{-1}$, and the barrier location and height decrease as $r_B(\sigma) \approx 8(\rho/\rho_c - 1)/\pi \tilde{\sigma}$ and $F_B \approx 2(1 - \rho/\rho_c) \log \tilde{\sigma}$, respectively, where $\tilde{\sigma} \equiv \sigma L^3 / k_B T$.

Two features of the stress-dependent confinement potential can have dramatic consequences for the long-time dynamics. First, as is implicit in the above and explicitly shown in the inset of Fig. 2, at fixed density the most probable (and the mean) transient localization length grows with increasing σ , corresponding to deformation-induced tube dilation. Within the phenomenological tube framework, conflicting arguments have been advanced that the tube diameter grows, shrinks, or remains unchanged under deformation.² We predict tube dilation, and the ratio of the tube radius at absolute yield to its quiescent value grows as $r_{l,yield}/r_l \sim \sqrt{\rho L^3}$ for $\rho \gg \rho_c$. Since in the static tube model (and dynamic theory^{9,10}) the rotational diffusion constant $D_{rot} \propto D_{\perp} \propto (r_l/L)^2$, tube dilation results in a significant acceleration of reptative relaxation, especially for heavily entangled solutions near σ_y . Second, as shown in Fig. 2, since F_B decreases rapidly with stress, a deformation-assisted transverse barrier hopping process emerges as a parallel relaxation channel which competes with reptation.

The average activated transverse barrier hopping time is computed from Kramers’ mean first-passage time result¹⁴

$$\frac{\tau_{\perp,hop}}{\tau_0} = \frac{2\pi}{\sqrt{K_0 K_B}} e^{\beta F_B}, \quad (2)$$

where K_0 and K_B are the absolute magnitudes of the local curvatures at the confinement potential minimum and barrier location, respectively, and $\tau_0 = L^2/D_{||,0}$ is proportional to the

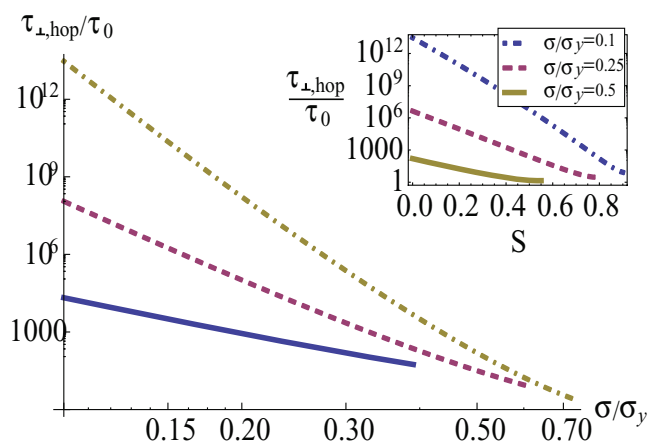


FIG. 3. Log-log plot of the dimensionless transverse hopping time vs. normalized stress for $\rho/\rho_c = 3, 6, 10$ (bottom to top). Each curve has been terminated at the stress where $F_B \approx 2k_B T$. Inset: Log-linear plot of the transverse hopping time vs. orientational order parameter for $\rho/\rho_c = 10$ at different fixed stresses.

fast (dilute-solutionlike for rods¹) CM longitudinal translation “reptation time,” which is far shorter than its transverse analog or the rotation time.^{1,10} Figure 3 illustrates the drastic decrease of the transverse hopping time with increasing stress. As a consequence of the large-displacement logarithmic growth of the quiescent confinement potential (and concomitant logarithmic decay of F_B with σ), the hopping time decreases as a power law for relatively small stresses with a ρ -dependent exponent: $\tau_{\perp, \text{hop}} \propto (\sigma/\sigma_y)^{-\theta}$, where $\theta = 2(\rho/\rho_c - 1)$. As $\sigma \rightarrow \sigma_y$, $F_B \rightarrow 0$, and $\tau_{\perp, \text{hop}}$ must smoothly recover its “bare” value,¹⁵ $\tau_{\perp, \text{hop}} \rightarrow \tau_0$. In practice, Eq. (2) is not valid as barriers approach the thermal energy, and thus the curves in Figs. 3 and 4 are shown only for $F_B \geq 2k_B T$.

The quiescent reptation-controlled rotational relaxation time is $\tau_{\text{rot}}(\rho) = (\tau_0/36) \cdot (D_{\perp}(\rho)/D_{\perp,0})^{-1}$. Due to the competition between reptation and activated transverse hopping we predict three distinct dynamical regimes. For σ/σ_y suf-

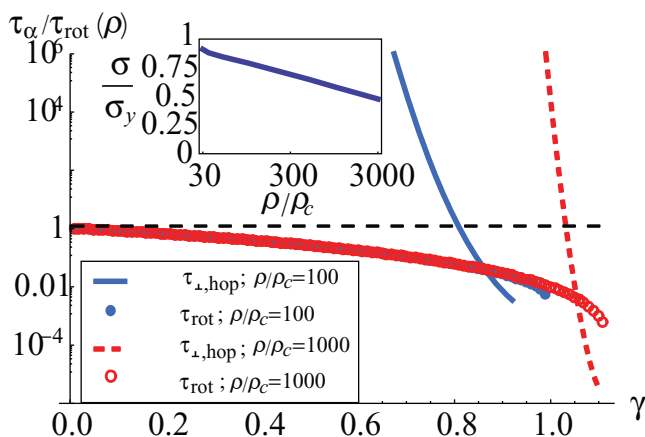


FIG. 4. Log-linear plot of initial relaxation times normalized by the quiescent rotational relaxation time vs. strain under instantaneous step-strain conditions. The dashed horizontal line indicates the unperturbed reptation behavior. Inset: Linear-log plot of normalized stress at the onset of the dynamic yielding regime (defined by $\tau_{\perp, \text{hop}}(\sigma) = \tau_{\text{rot}}(\sigma)$) vs. dimensionless density in the absence of rod alignment.

ficiently less than unity, the hopping time is astronomically long relative to τ_{rot} , and hence the basic reptation-tube picture remains unchanged. In the opposite limit where $\sigma/\sigma_y > 1$, a microscopic “elastic instability”-like phenomenon is predicted, defined by the complete destruction of tube constraints. A third dynamical regime emerges at high-enough densities over an intermediate range of stresses, in which the entropic barrier still exists but it is small enough that $\tau_{\perp, \text{hop}} < \tau_{\text{rot}}$. This regime occurs when, on average, the stress causes the entanglement network to collapse before deformation-accelerated reptative relaxation is completed. The normalized stress at the onset of this regime is plotted in the inset of Fig. 4 and depends only weakly on degree of entanglement, decreasing at high rod densities as either as an apparent logarithm or low-exponent power law.

In reality, deformation results in an external torque on polymers, which induces rod alignment. As previously discussed,⁹ this can be included via an Onsager-like distribution¹ for the relative orientation of two rods: $f(\mu, \alpha) = \alpha \cosh(\mu\alpha)/4\pi \sinh \alpha$, where α parameterizes the degree of orientation relative to some axis and μ is the dot product of the orientation vectors of the two rods. In terms of the nematic order parameter, $S = \langle (3\cos^2\theta - 1)/2 \rangle$, we find the effect of alignment is well described as a reduction of the effective density by a factor of $\sqrt{1-S}$. Since ρ enters the exponent of the transverse hopping time, rod alignment can enormously speed up lateral disentanglement, as illustrated for fixed density and stress in the inset of Fig. 3.

To explicitly demonstrate enhanced dynamical tube destruction due to coupling of stress and orientation, we compute the two mean relaxation times immediately after an instantaneous shear strain of dimensionless amplitude γ . Assuming an affine deformation, rods rotate and the shear stress is $\sigma(t=0^+) = 3\rho k_B T \gamma / (5 + \gamma^2)$.¹ The Lodge-Meissner relation¹ can be used to relate the alignment angle to shear and normal stresses to obtain $S(t=0^+) = 2(-1 + 3\sqrt{1 + 4\gamma^{-2}})^{-1}$. Figure 4 plots the mean initial transverse barrier hopping and terminal rotational relaxation times, each normalized by the longest quiescent relaxation time, $\tau_{\text{rot}}(\rho)$. The massive reduction of $\tau_{\perp, \text{hop}}$ relative to the comparatively weak tube-dilation effect on the rotational relaxation time is evident. Even for $\rho/\rho_c \sim 100 - 1000$, very high degrees of entanglement relevant to solutions of synthetic rods or stiff biopolymers,¹⁶ entropic barriers can become sufficiently low that transverse hopping becomes faster than (tube-dilated) reptation at strains of order unity, well below the “over-orientation” stress maximum at $\gamma = \sqrt{5}$.¹

In conclusion, our most important prediction for the transverse confinement potential in entangled liquids is that the confining tube has a finite strength which has many dramatic and novel consequences. Applied stress and induced polymer alignment can result in a dramatic acceleration of terminal relaxation not anticipated by the reptation-tube approach. With increasing stress we predict: (i) the tube widens, resulting in reduced entanglement and faster reptative relaxation, in qualitative agreement with a recent chain polymer simulation,⁴ (ii) a transverse activated barrier hopping relaxation process then emerges that can become faster than (tube-dilated) reptation, and (iii) the tube is completely destroyed

(microscopic absolute yielding) for $\sigma > \sigma_y$. The latter two regimes appear to be qualitatively consistent (at zeroth order) with recent experimentally based suggestions that tubes can become severely weakened or destroyed by stress,^{5,6} and also the observation of yield strains of order unity for rigid rod (microtubules)¹⁷ and flexible chain liquids.⁶ Although at present there is a dearth of data on isotropic, high-aspect-ratio rod solutions under deformation, our predictions can be directly tested by new simulations and creep experiments. Moreover, the present work provides a foundation for developing molecular-based constitutive equations for rheological response under step-strain and startup continuous shear conditions, a direction of our ongoing work. We anticipate our ideas will also be relevant to non-reptating branched polymers⁴ and chain liquids.

This work was supported by the Nanoscale Science and Engineering Initiative of the National Science Foundation under NSF Award No. DMR-0642573.

¹M. Doi and S. F. Edwards, *The Theory of Polymer Dynamics* (Oxford University, Oxford, 1986)

- ²T. C. B. McLeish, *Adv. Phys.* **51**, 13709 (2002).
- ³G. Marrucci, *J. Non-Newtonian Fluid Mech.* **62**, 279 (1996).
- ⁴A. Kushwaha and E. S. G. Shaqfeh, *J. Rheol.* **55**, 463 (2011).
- ⁵S. Ravindranath and S. Q. Wang, *J. Rheol.* **52**, 957 (2008).
- ⁶S. Q. Wang, S. Ravindranath, Y. Wang, and P. Boukany, *J. Chem. Phys.* **127**, 064903 (2007); Y. Wang and S. Q. Wang, *J. Rheol.* **53**, 1389 (2009).
- ⁷A. E. Likhtman, *J. Non-Newtonian Fluid Mech.* **157**, 158 (2009); R. G. Larson, *J. Polym. Sci., Part B: Polym. Phys.* **45**, 3240 (2007).
- ⁸D. M. Sussman and K. S. Schweizer, *Phys. Rev. E* **83**, 061501 (2011).
- ⁹D. M. Sussman and K. S. Schweizer, *Phys. Rev. Lett.* **107**, 078102 (2011).
- ¹⁰G. Szamel, *Phys. Rev. Lett.* **70**, 3744 (1993); G. Szamel and K. S. Schweizer, *J. Chem. Phys.* **100**, 3127 (1994).
- ¹¹B. Wang, J. Guan, S. M. Anthony, S. C. Bae, K. S. Schweizer, and S. Granick, *Phys. Rev. Lett.* **104**, 118301 (2010).
- ¹²V. Kobaev and K. S. Schweizer, *Phys. Rev. E* **71**, 021401 (2005).
- ¹³E. J. Saltzman, G. Yatsenko, and K. S. Schweizer, *J. Phys.: Condens. Matter* **20**, 244129 (2008); K. Chen, E. J. Saltzman, and K. S. Schweizer, *Annu. Rev. Condens. Matter Phys.* **1**, 277 (2010).
- ¹⁴P. Hänggi, P. Talkner, and M. Borkovec, *Rev. Mod. Phys.* **62**, 251 (1990).
- ¹⁵E. J. Saltzman and K. S. Schweizer, *J. Chem. Phys.* **125**, 044509 (2006).
- ¹⁶D. C. Morse, *Phys. Rev. E* **63**, 031501 (2001).
- ¹⁷Y. C. Lin, G. H. Koenderink, F. C. MacKintosh, and D. A. Weitz, *Macromolecules* **40**, 7714 (2007).